

# Mechanistic Studies on the Copper-Catalyzed Hydrosilylation of Ketones

Jean-Thomas Issenhuth,<sup>[a]</sup> François-Paul Notter,<sup>[b]</sup> Samuel Dagorne,<sup>[a]</sup> Alain Dedieu,<sup>\*,[b]</sup> and Stéphane Bellemin-Laponnaz<sup>\*,[a]</sup>

**Keywords:** Density functional calculations / Mechanistic studies / Asymmetric catalysis / Hydrosilylation / Copper

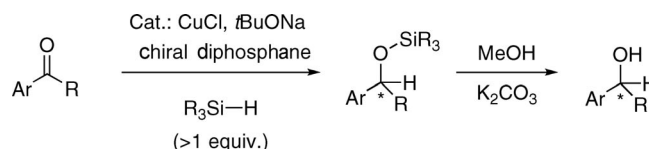
The copper-catalyzed asymmetric hydrosilylation of ketones is an efficient method for the synthesis of chiral enantiopure secondary alcohols. Herein, we present a detailed computational study (DFT/B3LYP) of the copper(I)-catalyzed reaction. In particular, the two transition states involved in the catalytic cycle have been determined. The insertion of the ketone into the Cu–H bond was found to have a lower activation

barrier than the reaction of the copper alkoxy intermediate with the silane, which regenerates Cu–H along with the silyl ether product. Our findings also reveal the importance of the copper hydride dimer in controlling the reactivity toward the ketone. The conclusions are supported by experimental mechanistic investigations including kinetic studies, kinetic isotope effect, and isotope labeling measurements.

## Introduction

Asymmetric hydrosilylation of ketones with silane (Si–H) catalyzed by chiral transition-metal complexes followed by hydrolysis provides an efficient route to chiral enantiopure secondary alcohols. It is considered as an alternative to asymmetric hydrogenation to access such molecules.<sup>[1,2]</sup> The first examples<sup>[3]</sup> in the early 1970s provided the basis for the development of efficient rhodium-based catalysts with chiral phosphanes, nitrogen-, or sulfur-containing ligands, several of which afforded products with enantiomeric excesses above 90%.<sup>[4,5]</sup> Efficient systems using less expensive metals such as ruthenium,<sup>[6]</sup> zinc,<sup>[7]</sup> titanium,<sup>[8]</sup> or iron<sup>[9]</sup> have been used with success.<sup>[10]</sup> Brunner and Miehl reported in 1984 the first example of copper-catalyzed asymmetric hydrosilylation.<sup>[11]</sup> They found that a catalytic amount of copper hydride in the presence of the DIOP ligand promoted the hydrosilylation of acetophenone. Although the enantioselectivities were found to be low (*ee* values up to 39%), these results first established that copper/diphosphane systems were promising catalysts for this type of reaction. In 2001, Lipshutz et al. reported that the combination of the bidentate phosphane 3,5-xyl-MeO-BIPHEP with copper hydride is an efficient catalyst for the hydrosilylation of ketones (Scheme 1).<sup>[12,13]</sup> The active species of the system was formed in situ by the now well-established procedure involving CuCl, NaOtBu, and diphosphane

(Scheme 2).<sup>[10c,14]</sup> High levels of enantioselectivity were observed with a low catalyst loading and under mild conditions. Moreover, polymethylhydrosiloxane (PMHS), an inexpensive silane, was used as a stoichiometric source of hydride. Lipshutz et al. later on established that bulky diphosphanes of the SEGPHOS family were also efficient ligands for the hydrosilylation reaction.<sup>[15]</sup> More recently, we reported that the commercially available chiral phosphane BINAP may be a suitable supporting ligand for highly enantioselective copper-catalyzed asymmetric hydrosilylation reactions of ketone substrates.<sup>[16]</sup>



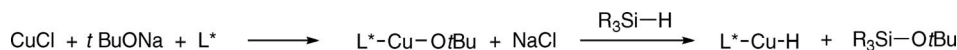
Scheme 1. Asymmetric hydrosilylation of aryl alkyl ketones with copper(I) as catalyst.

Surprisingly, there have been relatively few mechanistic investigations on these Cu/phosphane-mediated hydrosilylation reactions. It has been originally proposed that the mechanism by which the ketone undergoes stereoselective insertion into the Cu–H bond would involve a four-membered transition state. Another subsequent four-membered transition state between the formed copper alkoxy and silane Si–H would give the silyl ether as the product along with regeneration of the Cu–H species (Scheme 3). Lipshutz et al. investigated the nature of the reagent by spectroscopic and chemical means and found that the originally proposed catalytic cycle depicted in Scheme 3 does not explain several of the key observations.<sup>[15]</sup> In particular, no reaction was observed when a stoichiometric amount of (Ph<sub>3</sub>P)Cu–H along with 20 mol-% of BIPHEP ligand and propiophen-

[a] Laboratoire Decomet, Institut de Chimie, CNRS-Université de Strasbourg,  
1, rue Blaise Pascal, 67000 Strasbourg, France

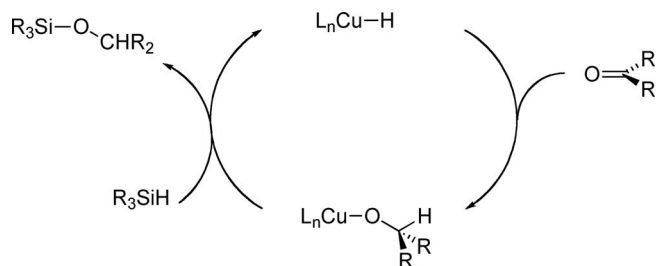
[b] Laboratoire de chimie quantique, Institut de Chimie, CNRS-Université de Strasbourg,  
1, rue Blaise Pascal, 67000 Strasbourg, France  
E-mail: bellemin@unistra.fr

Supporting information for this article is available on the WWW under <http://dx.doi.org/10.1002/ejic.200900961>.



Scheme 2. In situ generation of the active Cu–H catalyst.

one were mixed in the absence of a silane (Scheme 4). Subsequent addition of PMHS to the reaction mixture afforded the expected secondary alcohol in high yield. On the basis of these results, a silyl hydrido cuprate (**A**, Scheme 4) was conjectured as the active species rather than a discrete copper hydride/diphosphane system.



Scheme 3. Originally proposed catalytic cycle.

On the basis of our studies on the copper-catalyzed hydrosilylation reaction (with BINAP as the ligand), we reached the same conclusion, i.e., the silane is most likely an integral part of the catalyst. These preliminary studies prompted us to propose either a pentacoordinate silicon intermediate of type **B** or a copper(III) intermediate of type **C** as the active species.<sup>[17]</sup> However, further studies were clearly needed to fully understand the mechanistic pathway.

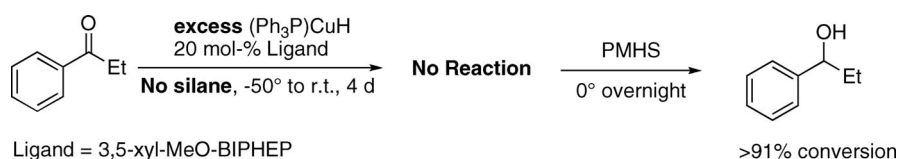
In order to provide a rational catalytic cycle of the copper-catalyzed hydrosilylation of ketones, we have further investigated the mechanism of this reaction. We report here the results of these detailed mechanistic studies, which combine DFT calculations, kinetic studies, kinetic isotope effect (KIE) studies, and isotope labeling studies.<sup>[18]</sup> They all support – with some supplementary details – the catalytic cycle that was originally suggested.

## Results

### Theoretical Studies

DFT-B3LYP calculations were carried out on models of increasing complexity for the catalyst, namely Cu(H)(PH<sub>3</sub>)<sub>2</sub> (**1a**), Cu(H)[H<sub>2</sub>P(C<sub>4</sub>H<sub>4</sub>)PH<sub>2</sub>] (**1b**), Cu(H)[H<sub>2</sub>P(C<sub>12</sub>H<sub>8</sub>)PH<sub>2</sub>] (**1c**), and Cu(H)[Ph<sub>2</sub>P(C<sub>12</sub>H<sub>8</sub>)PPh<sub>2</sub>] (**1d**). As the four models turned out to yield similar results,<sup>[19]</sup> we will concentrate here on systems that lie at the two ends of this complexity scale, namely Cu(H)(PH<sub>3</sub>)<sub>2</sub> (**1a**) and Cu(H)[Ph<sub>2</sub>P(C<sub>12</sub>H<sub>8</sub>)PPh<sub>2</sub>] (**1d**). The ketone was modeled by either acetone or acetophenone, and the silane by SiH<sub>2</sub>Me<sub>2</sub>. Note that we considered for **1d** a (*R*)-[Ph<sub>2</sub>P(C<sub>12</sub>H<sub>8</sub>)PPh<sub>2</sub>] ligand, as in the experimental studies. For the sake of simplicity, we will denote in the following the (*R,R*) and (*R,S*) diastereoisomers of the products, intermediates, and transition states by (*R*) and (*S*) respectively, according to the chirality of the carbon atom of the acetophenone.

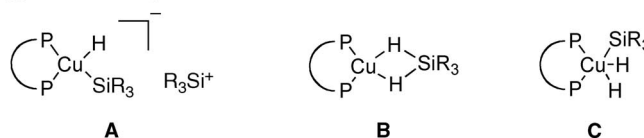
The energetic results obtained for the reactants, intermediates, transition states, and products of the conventional catalytic cycle (Scheme 3), with catalysts **1a** and **1d**, are summarized in Table 1. The corresponding free energy profile for **1d** and acetone is given in Figure 1. Starting from the three model reactants, namely the bis(phosphane) copper hydride catalyst, Me<sub>2</sub>CO, and SiH<sub>2</sub>Me<sub>2</sub>, we first obtained a weak adduct between the copper complex and acetone, with a stabilization enthalpy of 5.1 and 6.3 kcal mol<sup>−1</sup> for **1a** and **1d**, respectively. Note that this precursor is somewhat destabilized with respect to the reactants when entropic effects are taken into account with the underlying assumption that all molecules are in the gas phase (Table 1). Such an assumption is known to yield an entropy decrease that is too large, however, and the true Δ*G* value for the adduct lies more likely closer to the Δ*E* or Δ*H* values.<sup>[20]</sup>



Ligand = 3,5-xyl-MeO-BIPHEP

&gt;91% conversion

Suggested active species:



Scheme 4. Impact of the silane on ketone reduction and suggested active species that may explain the unexpected unreactivity of CuH with propiophenone.

We also found other adducts with various geometries between the copper complex and  $\text{SiH}_2\text{Me}_2$ , but their stabilization energy was smaller by about  $4 \text{ kcal mol}^{-1}$  (vide infra). The geometry of the [bis(phosphane)copper hydride]... $\text{Me}_2\text{CO}$  adduct does not correspond to a copper–ketone  $\pi$  complex, because, as shown in Figure 2, the  $\text{C}=\text{O}$  bond and

the  $\text{Cu}-\text{H}$  bonds are almost coplanar (the  $\text{O}-\text{C}-\text{Cu}-\text{H}$  dihedral angle is  $7.4^\circ$ ). The oxygen atom sits at the apex of the copper, and the carbon atom is at the apex of the hydride, the corresponding distances being  $3.207 \text{ \AA}$  and  $3.170 \text{ \AA}$ , respectively. These values show that the  $\text{Cu}-\text{O}$  bond is not made yet and that the geometry is more likely due to di-

Table 1. Free energy differences and enthalpy differences (in  $\text{kcal mol}^{-1}$ ) between the reactants and the intermediates and transition states of the hydrosilylation reactions of acetone and acetophenone catalyzed by  $[\text{Cu}(\text{H})(\text{PH}_3)_2]$  (**1a**) and  $\text{CuH}[\text{Ph}_2\text{P}(\text{C}_{12}\text{H}_8)\text{PPh}_2]$  (**1d**). The model silane is  $\text{SiH}_2\text{Me}_2$  in both cases. The zero of energy refers to the separated reactants.

$\text{R}_2 = (\text{CH}_3)_2$	<b>1a</b> $\Delta G$	$\Delta H$	<b>1d</b> $\Delta G$	$\Delta H$
$\text{CuHL}_2 + \text{R}_2\text{CO} + \text{SiH}_2\text{Me}_2$	0.0 <sup>[a]</sup>	0.0	0.0 <sup>[a]</sup>	0.0
$\text{CuHL}_2 \cdots \text{R}_2\text{CO} + \text{SiH}_2\text{Me}_2$	+4.4	−5.1	+5.3	−6.3
$\text{TS1} + \text{SiH}_2\text{Me}_2$	+15.6	+1.5	+13.8	−2.1
$\text{CuL}_2(\text{OCHR}_2) + \text{SiH}_2\text{Me}_2$	−6.5	−18.9	−8.7	−22.3
$\text{CuL}_2(\text{OCHR}_2) \cdots \text{SiH}_2\text{Me}_2$	−0.7	−22.2	−	−
$\text{TS2}$	+24.3	−4.1	+28.4	−0.4
$\text{CuHL}_2 \cdots (\text{HMe}_2\text{SiOCHR}_2)$	−7.3	−30.5	−	−
$\text{CuHL}_2 + (\text{HMe}_2\text{SiOCHR}_2)$	−16.1	−28.7	−16.1	−28.7
$\text{R}_2 = (\text{CH}_3)(\text{C}_6\text{H}_5)$	<b>1a</b> $\Delta G$	$\Delta H$	<b>1d</b> $\Delta G$	$\Delta H$
$\text{CuHL}_2 + \text{R}_2\text{CO} + \text{SiH}_2\text{Me}_2$	0.0 <sup>[b]</sup>	0.0	0.0 <sup>[b]</sup>	0.0
$\text{CuHL}_2 \cdots \text{R}_2\text{CO} + \text{SiH}_2\text{Me}_2$	+5.5	−4.1	+6.7 (R), +6.1 (S)	−4.5 (R), −4.4 (S)
$\text{TS1} + \text{SiH}_2\text{Me}_2$	+16.1	+2.8	+15.3 (R), +16.0 (S)	+0.3 (R), +1.6 (S)
$\text{CuL}_2(\text{OCHR}_2) + \text{SiH}_2\text{Me}_2$	−7.3	−18.5	−9.5 (R), −8.1 (S)	−23.4 (R), −20.3 (S)
$\text{CuL}_2(\text{OCHR}_2) \cdots \text{SiH}_2\text{Me}_2$	−0.3	−21.3	−	−
$\text{TS2}$	+25.1	−1.3	+31.0 (R), +24.4 (S)	3.5 (R), −2.9 (S)
$\text{CuHL}_2 \cdots (\text{HMe}_2\text{SiOCHR}_2)$	−2.1	−25.8	−	−
$\text{CuHL}_2 + (\text{HMe}_2\text{SiOCHR}_2)$	−14.4	−25.9	−14.4 (R), −14.4 (S)	−25.9 (R), −25.9 (S)

[a] The sum of the B3LYP total free energies (in au) of the reactants **1** +  $(\text{CH}_3)_2\text{CO}$  +  $\text{SiH}_2\text{Me}_2$  are: −2890.79617 (for **1a**), −4275.48940 (for **1d**). [b] The sum of the B3LYP total free energies (in au) of the reactants **1** +  $\text{CH}_3\text{COC}_6\text{H}_5$  +  $\text{SiH}_2\text{Me}_2$  are: −3082.48563 (for **1a**), −4467.17886 (for **1d**).

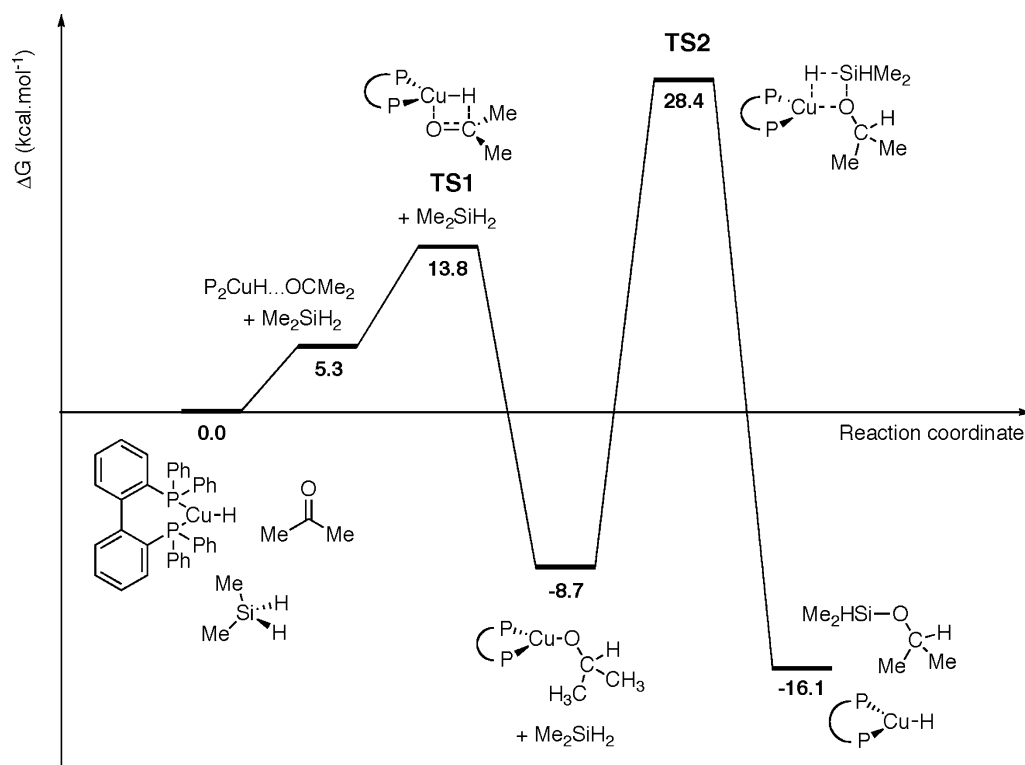


Figure 1. Free energy profile for the hydrosilylation reaction of  $\text{Me}_2\text{SiH}_2$  with  $\text{Me}_2\text{CO}$  catalyzed by  $[\text{Ph}_2\text{P}(\text{C}_{12}\text{H}_8)\text{PPh}_2]\text{CuH}$ .

polar attractive interactions. However, the copper complex and the ketone are perfectly aligned to undergo the insertion process that leads to the alkoxy  $\text{CuL}_2\text{-(OCHMe}_2\text{)}$  intermediate. Despite its  $\sigma^2 + \pi^2$  nature, which makes it formally forbidden in the Woodward–Hoffmann sense, the one-step process in this weak precursor is relatively easy: the computed free energy barrier from the separated reactants is 15.6 and 13.8 kcal mol<sup>-1</sup> for **1a** and **1d**, respectively. Similar values are found when the ketone is acetophenone. As shown in the interaction diagram in Figure 3 (based on a thorough analysis of the wave function), this relatively low barrier is the result of a two-electron stabilizing interaction between the empty  $\pi^*$  orbital of the ketone and the doubly occupied Cu–H  $\sigma$ -bond orbital that more or less counteracts the four-electron repulsive interaction between the doubly occupied  $\pi$  orbital of acetone and the doubly occupied  $\sigma^*$ -bond orbital of Cu–H. As far as the enantioselectivity of this step is concerned and in the case of the reaction of **1d** with acetophenone, one may note that the most stable diastereoisomeric form of the transition state [the (*R*) one] leads to the most stable diastereoisomer for the alkoxy intermediate. Figure 4 shows these (*R*) and (*S*) transition states. In the (*R*) transition state, the acetophenone comes slightly closer to the copper hydride complex than in the (*S*) transition state: the Cu···O and H···C distances are to 2.35 Å and 1.87 Å, respectively, in the (*R*) form and 2.37 and 1.90 Å, respectively, in the (*S*) form. One also finds shorter distances between the phenyl group of acetophenone and the *ortho* and *meta* hydrogen atoms of the phenyl group in the [Ph<sub>2</sub>P(C<sub>12</sub>H<sub>8</sub>)PPh<sub>2</sub>] ligand.

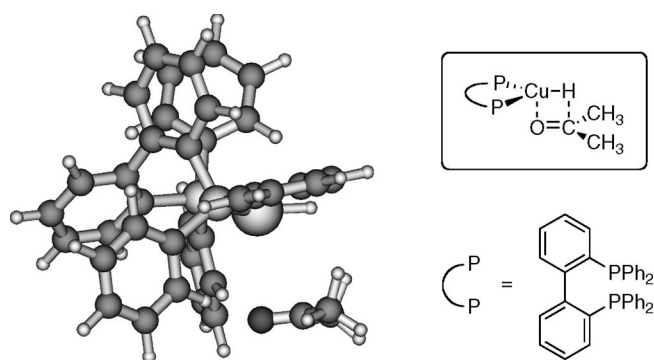


Figure 2. Optimized structures (DFT-B3LYP/BSI) of the adduct between acetone and [Ph<sub>2</sub>P(C<sub>12</sub>H<sub>8</sub>)PPh<sub>2</sub>]CuH.

The alkoxy complex may then very weakly interact with the silane before undergoing the  $\sigma$ -bond metathesis that yields the silyl ether product and restores the Cu(H)L<sub>2</sub> catalyst. We again found an adduct between the alkoxy intermediate and the silane for both Cu(PH<sub>3</sub>)<sub>2</sub>(OCHMe<sub>2</sub>) and Cu(PH<sub>3</sub>)<sub>2</sub>(OCHC<sub>6</sub>H<sub>5</sub>Me), stabilized by a few kcal mol<sup>-1</sup> ( $\Delta H$  value, see Table 1). We did not optimize such an adduct in the case of catalyst **1d**, because of the computational time required, but one may reasonably expect its presence from the similar results found for **1a** and **1d** for the other results (Table 1). The  $\sigma$ -bond metathesis step appears to be driven by the formation of the silyl ether product: the coupling between Me<sub>2</sub>CO and SiH<sub>2</sub>Me<sub>2</sub> is exoergic by

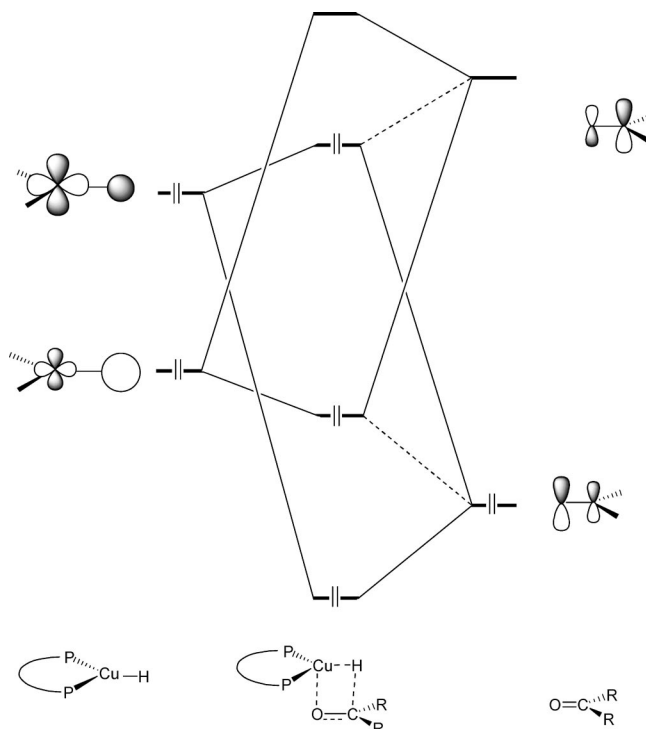


Figure 3. Orbital interaction diagram between the frontier orbitals of the bis(phosphane) copper hydride complex and of a ketone.

16.1 kcal mol<sup>-1</sup>. Yet the associated barrier is relatively high, especially in the case of the more realistic **1d** catalyst (see Table 1 and Figure 1). The corresponding transition state is the highest point on the whole energy profile, 31.0 and 24.4 kcal mol<sup>-1</sup> above the separated reactants for the coupling reaction between C<sub>6</sub>H<sub>5</sub>MeCO and SiH<sub>2</sub>Me<sub>2</sub> catalyzed respectively by the *R* and *S* enantiomers of Cu(H)-[Ph<sub>2</sub>P(C<sub>12</sub>H<sub>8</sub>)PPh<sub>2</sub>] (Table 1). This rather high barrier is best explained, as shown in the schematic interaction diagram in Figure 5, by a four-electron destabilizing interaction between the double d<sub>z<sup>2</sup></sub> orbital of CuL<sub>2</sub>(OCHR<sub>2</sub>) and a Si–H bonding orbital of SiH<sub>2</sub>Me<sub>2</sub> (based again on a thorough analysis of the wave function). There is also a four-electron destabilizing interaction between the HOMO of the SiH<sub>2</sub>Me<sub>2</sub> and the out-of-plane lone pair of the OCHR<sub>2</sub> ligand, but the antibonding combination of these two orbitals is stabilized by an in-phase mixing of the LUMO of the deformed silane. It is interesting to note here that the deformation around the silicon atom in the transition state is such that one gets a trigonal-bipyramidal geometry, known to be a stable geometry for pentavalent silicon compounds.<sup>[21]</sup> Indeed, as shown in the Scheme 5, the three-orbital mixing depicted in Figure 5 yields for the HOMO of the transition state the typical nonbonding orbital of such compounds.<sup>[22]</sup> The relative facility of Si to achieve hypervalency, also from a steric point of view,<sup>[23]</sup> is therefore one of the factors that accounts for a barrier not too high in energy.

Figure 6 shows the optimized geometries, in the case of **1d**, for the two diastereoisomeric forms of transition state **TS2**. In contrast to the results obtained for **TS1**, there is

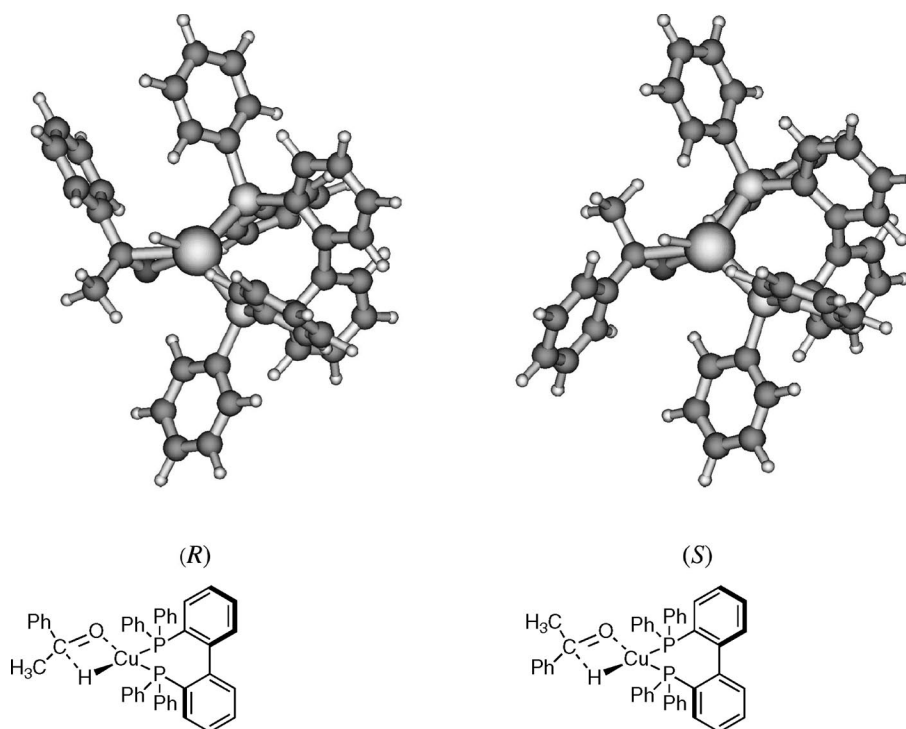


Figure 4. Optimized structures (DFT-B3LYP/BSI) of the (*R*) and (*S*) transition states for the insertion of acetophenone in the Cu–H bond of  $[\text{Ph}_2\text{P}(\text{C}_{12}\text{H}_8)\text{PPh}_2]\text{CuH}$ .

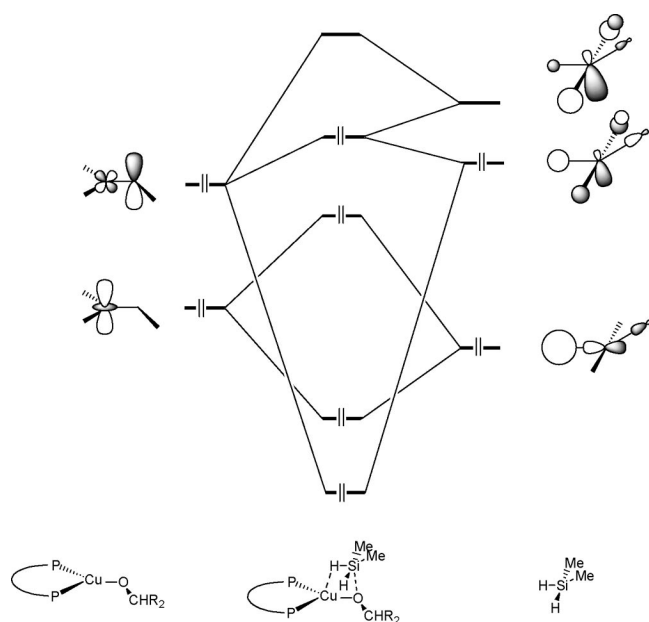
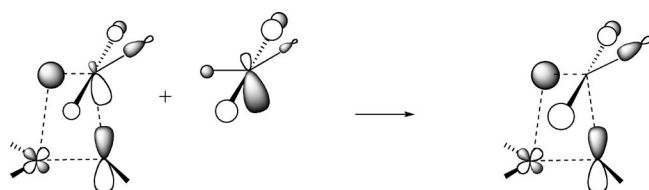


Figure 5. Orbital interaction diagram between the frontier orbitals of  $[\text{Ph}_2\text{P}(\text{C}_{12}\text{H}_8)\text{PPh}_2]\text{CuOCHR}_2$  and  $\text{SiH}_2\text{Me}_2$ .



Scheme 5.

now a rather large energy separation between these two, the (*R*) diastereoisomeric form being destabilized with respect to the (*S*) diastereoisomeric form by more than  $6 \text{ kcal mol}^{-1}$ , regardless of whether entropic effects are taken into account (see Table 1). Figure 6 clearly shows the main reason for this destabilization: In the (*S*) form, the phenyl ring of the phenylethoxy ligand and the O–C bond are roughly coplanar (the O–C–*C*<sub>ortho</sub>–H<sub>ortho</sub> dihedral angle is  $-19.7^\circ$ ), due to the existence of a hydrogen bond between the *ortho* hydrogen of the phenyl ring and the oxygen atom. In the (*R*) form, the *ortho* hydrogen atom cannot form such a hydrogen bond because of strong steric repulsions of this phenyl ring with one of the phenyl rings of the ancillary  $[\text{Ph}_2\text{P}(\text{C}_{12}\text{H}_8)\text{PPh}_2]$  diphosphane ligand (the one at the rear, almost hidden by the Cu–O bond in Figure 6). The phenyl group of the phenylethoxy ligand is therefore turned up, the O–C–*C*<sub>ortho</sub>–H<sub>ortho</sub> dihedral angle now being  $53.2^\circ$ . Note that such a discriminating feature is not present for the **TS1** transition state, in which the acetophenone moiety has, as expected,<sup>[24–26]</sup> its phenyl ring and the C=O bond roughly coplanar in both (*R*) and (*S*) forms (see Figure 4). Quite interesting is also the fact that in gaseous acetophenone the experimental and theoretical values for the torsional barrier around the C<sub>phenyl</sub>–C<sub>carbonyl</sub> bond range between  $3.1$  and  $5.6 \text{ kcal mol}^{-1}$ .<sup>[21,22]</sup>

From the results in Table 1, it is also clear that the energetic results do not change appreciably on going from  $\text{L}_2 = (\text{PH}_3)_2$  to  $\text{L}_2 = [\text{Ph}_2\text{P}(\text{C}_{12}\text{H}_8)\text{PPh}_2]$  and on going from acetone to acetophenone. The same is true for the results, not reported here, that were obtained for the two other models of the catalysts.<sup>[17]</sup> One finds some variations, but they do



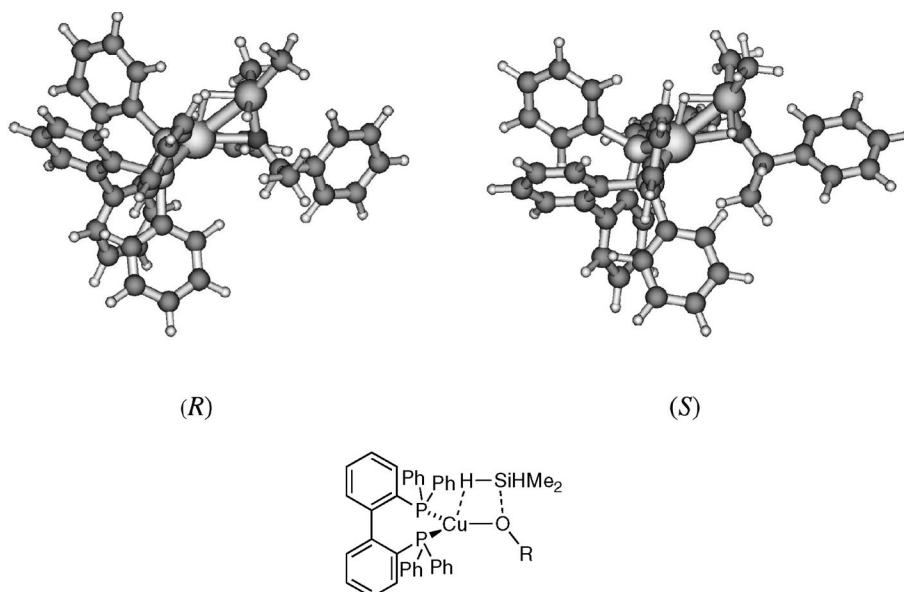


Figure 6. Optimized structures (DFT-B3LYP/BSI) of the (*R*) and (*S*) transition states for the insertion of  $\text{SiH}_2\text{Me}_2$  in the Cu–O bond of  $[\text{Ph}_2\text{P}(\text{C}_{12}\text{H}_8)\text{PPh}_2]\text{Cu}-\text{OCHMePh}$ .

not exceed a few  $\text{kcal mol}^{-1}$ . In particular, the second step remains the most difficult step. At this stage one may stress that improving the size of the basis set and/or taking into account the scalar relativistic effect by the use of a pseudopotential also did not alter our conclusions. This is best exemplified by the values obtained with BSII, BSIII, or BSIV for the first step of the reaction with **1a** or **1b** (Table S1 of the Supporting Information). We also carried out CCSD(T) single-point calculations for the  $\text{Cu}(\text{H})(\text{PH}_3)_2 \cdots \text{OCMe}_2 \rightarrow \text{Cu}(\text{PH}_3)_2(\text{OCHMe}_2)$  acetone insertion reaction and found no influence of the basis set and a de-

crease in the energy barrier by a few  $\text{kcal mol}^{-1}$  only (see Table S1). Moreover, recent calculations performed for various isomers of  $[\text{Cu}(\text{PhOH})]^+$  did not reveal severe discrepancies with the results obtained at the DFT and CCSD(T) levels.<sup>[27]</sup>

As far as the reaction mechanism is concerned, we checked (for **1a**) our previous suggestion that a pentacoordinate silicon intermediate of type **B** or a copper(III) intermediate like **C** might be involved (Scheme 4). We did not succeed in optimizing such intermediates. All attempts led invariably back to structures corresponding to  $\text{Cu}(\text{H})$ -

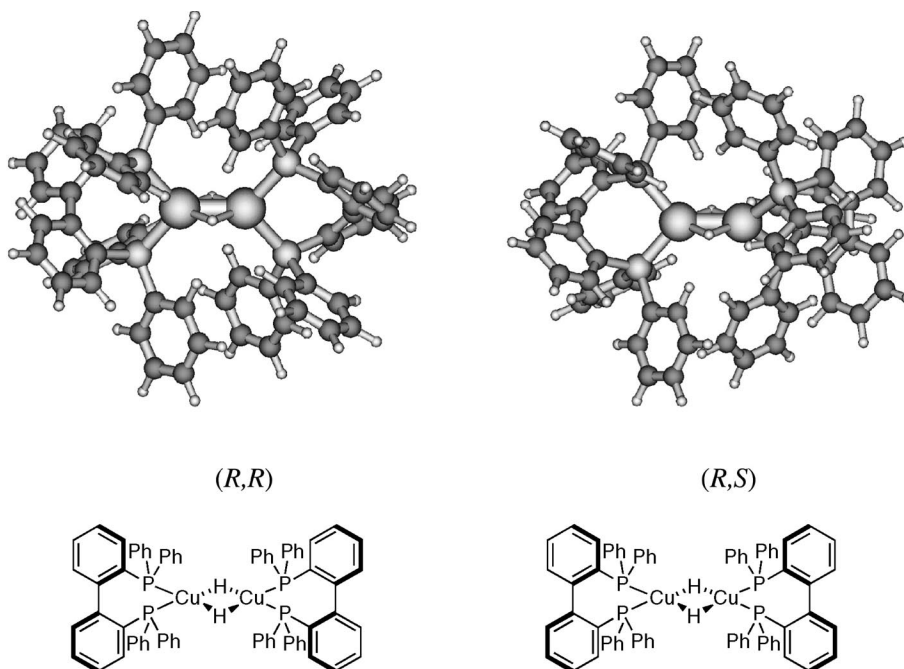


Figure 7. Optimized structures (DFT-B3LYP/BSI) of the (*R,R*) and (*R,S*)  $\{[\text{Ph}_2\text{P}(\text{C}_{12}\text{H}_8)\text{PPh}_2]\text{CuH}\}_2$  diastereoisomers.

$(\text{PH}_3)_2 + \text{SiH}_2\text{Me}_2$ , in which the silane interacts very weakly with the copper complex.<sup>[17]</sup> The stabilization energy for these adducts is found to range between 2.2 and 3.5 kcal mol<sup>-1</sup>, i.e., values which are even lower than that obtained for the adduct between  $\text{Cu}(\text{H})(\text{PH}_3)_2$  and  $\text{O}=\text{CMe}_2$ .

We finally investigated the dimer of catalyst **1d**,  $\{\text{Cu}(\text{H})[\text{Ph}_2\text{P}(\text{C}_{12}\text{H}_8)\text{PPh}_2]\}_2$ , for which two diastereoisomeric forms, either *R,R* or *R,S*, are possible. The optimized structures are shown in Figure 7. They are more stable than two monomers by 30.5 and 25.5 kcal mol<sup>-1</sup>, respectively ( $\Delta H$  value). These values are of course strongly reduced by entropic effects, down to 13.7 and 9.2 kcal mol<sup>-1</sup>. Note that taking into account basis set superposition error effects would reduce this value further. Quite interestingly too, the *R,R* diastereoisomer is more stable than the *R,S* diastereoisomer by 4.5 kcal mol<sup>-1</sup> ( $\Delta G$  value, the  $\Delta H$  value is 4.9 kcal mol<sup>-1</sup>), owing to less steric hindrance in the homochiral stereoisomer.

## Mechanistic Investigations

**Influence of the Temperature on the Selectivity:** The temperature dependence of the catalyst performance was studied for the hydrosilylation of acetophenone for the temperature range from -78 °C to 23 °C by using  $\text{CuCl}/\text{NaO}t\text{Bu}/(R)\text{-BINAP}$  as catalyst (5 mol-%) and  $(o\text{-tol})\text{PhSiH}_2$ ,  $\text{PhMeSiH}_2$ , or  $\text{Ph}_2\text{SiH}_2$  as the silane. In all cases, a linear relationship was observed between the temperature and the enantiomeric excess, which is consistent with a selectivity determining step that remains the same over the whole temperature range (see Figure S8 in the Supporting Information).

**Kinetic Studies:** In order to gain more insight into the mechanism, we conducted kinetic studies on two different catalytic systems, namely  $\text{CuCl}/\text{NaO}t\text{Bu}/\text{BINAP}$  and  $\text{CuCl}/\text{NaO}t\text{Bu}/\text{DMDP}$  [DMDP = 1,3-dimethyl bis(diphosphanyl)propane]. Conversion of acetophenone into the product was monitored by <sup>1</sup>H NMR spectroscopy as a function of time at a constant temperature with  $\text{PhMeSiH}_2$  as the hydride source. We then determined the initial rate values from an exponential fitting analysis of the conversion curves. For each component (silane, substrate, and precatalyst), we measured the initial rate at five different initial concentrations, while keeping the concentrations of the other reactants constant. Thus the kinetic dependence measured at 298 K in deuteriobenzene was found to obey first order in silane, first order in ketone, and half order in cata-

lyst. For example, Figure 8 displays the linear dependence between  $v_i$  and the square root of the total concentration of copper with DMDP as ligand, which indicates that a dimer most likely equilibrates with a small quantity of monomer catalyst, which is the active catalytic species. The same profile was confirmed with the BINAP ligand, which contradicts with our preliminary conclusions (conducted with less data).<sup>[16]</sup>

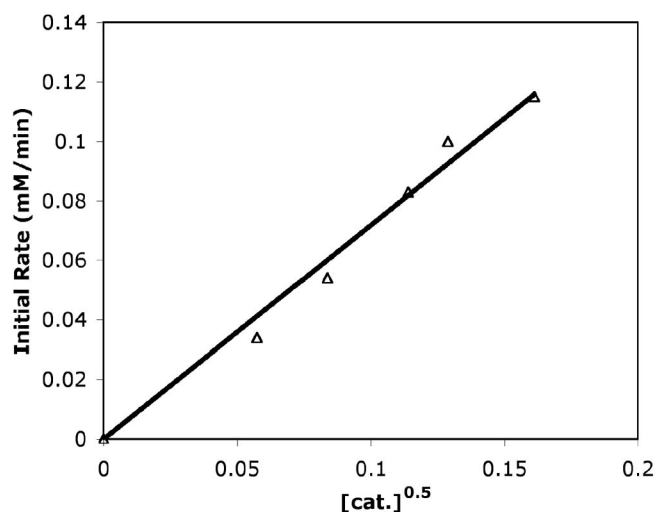
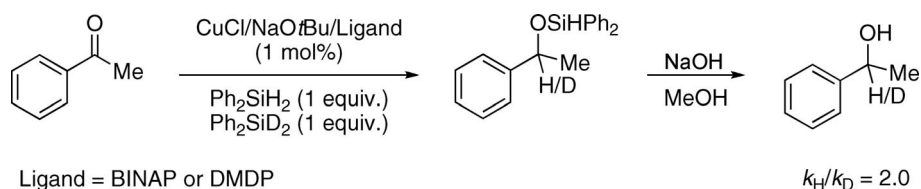


Figure 8. Plot of the initial rates of reaction (mM/min) vs. the square root of the initial concentration of copper/DMDP catalyst (mol/L). The initial concentrations of the other reactants were constant.

**Kinetic Isotope Effect:** The KIE in the hydrosilylation of acetophenone was also investigated with the two different diphosphanes. One equivalent of acetophenone was allowed to react with one equivalent of silane  $\text{Ph}_2\text{SiH}_2$  and one equivalent of the corresponding deuteriosilane  $\text{Ph}_2\text{SiD}_2$  by using the catalytic systems  $\text{CuCl}/t\text{BuONa}/\text{BINAP}$  or  $\text{CuCl}/t\text{BuONa}/\text{DMDP}$ . The degree of deuteration in the alcohol was determined by <sup>1</sup>H NMR spectroscopy. A product ratio of 2 to 1 for proton and deuterium incorporation, respectively, was measured, thus giving an isotope effect of  $k_{\text{H}}/k_{\text{D}} = 2.0$  (Scheme 6). In another experiment, we measured the initial rate values by using either  $\text{Ph}_2\text{SiH}_2$  or  $\text{Ph}_2\text{SiD}_2$  as a silane source and confirmed the  $k_{\text{H}}/k_{\text{D}}$  value: the ratio between the initial rates was found to be  $v_{i(\text{H})}/v_{i(\text{D})} = 2$ . This observed primary KIE is similar to that observed in the reduction of sulfoxide by silane, where the cleavage of a Si-H bond in a four-membered ring transition state is believed to be the rate determining step.<sup>[28]</sup> Chan and Zheng also

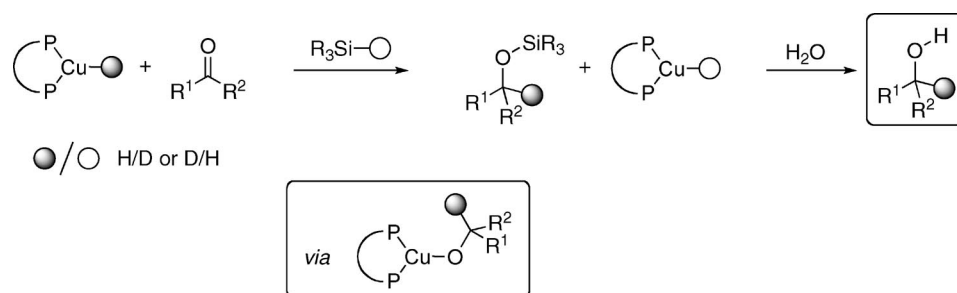


Scheme 6. Isotope effect on the hydrosilylation of acetophenone (solvent: toluene).

observed such a KIE in rhodium-catalyzed hydrosilylation, where the ketone inserts into the Si–H bond to yield an alkoxysilyl intermediate.<sup>[5b]</sup>

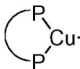
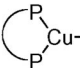
**Isotope Labeling:** To examine whether a discrete Cu–H species is the active intermediate that may interact with the ketone to form the corresponding copper alkoxide, we conducted several deuterium labeling studies. Indeed, on the basis of the originally proposed catalytic cycle, the Cu–H hydride should bind to the C=O carbon of the ketone substrate. Therefore, stoichiometric experiments that may provide support for this pathway were carried out. Reaction of a stoichiometric amount of LCu–H (L = diphosphane) with one equivalent of ketone and one equivalent of deuterated silane should lead to the hydrogenated product R<sup>1</sup>CH(OH)–R<sup>2</sup> (Scheme 7). On the other hand, the reaction of LCu–D with the ketone and hydrogenated silane should afford the deuterium-enriched product R<sup>1</sup>CD(OH)R<sup>2</sup>. Other suggested mechanistic pathways (i.e. Scheme 4) may lead to H/D scrambling with an H/D ratio resulting from the KIE. We conducted such experiments with BINAP and DMDP as phosphane ligands, and the results are summarized in

Table 2. When BINAP was used as ligand, the H/D ratio in the product was found to be independent of the reagents: H/D ratios of 64:36 and 60:40 were observed. In contrast, with DMDP as ligand, 80% hydrogen incorporation was observed with (DMDP)Cu–H as reagent and 76% deuterium incorporation was observed when (DMDP)Cu–D was used. Thus, whereas the use of DMDP as ligand cleanly confirms the classical pathway, that of BINAP leads to values close to the KIE. This different behavior may be explained by a possible scrambling of deuterium between LCu–H and Si–D (or LCu–D and Si–H), which can be considered as an interfering reaction (Scheme 8). We could quantify this scrambling rate by <sup>1</sup>H NMR spectroscopic kinetic studies. The reaction of H/D scrambling between Ph<sub>2</sub>SiD<sub>2</sub> and PhMeSiH<sub>2</sub> was studied in the presence of 1 mol-% of CuCl/NaOtBu/BINAP or CuCl/NaOtBu/DMDP in C<sub>6</sub>D<sub>6</sub> as solvent. It appeared that the H/D scrambling is much faster than the hydrosilylation reaction in the case of BINAP. The scrambling is somewhat less important with DMDP, which is consistent with the observed results.

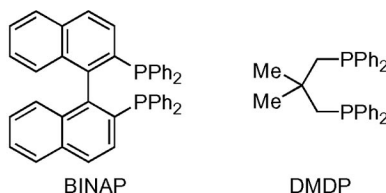


Scheme 7. Stoichiometric H/D labeling experiments.

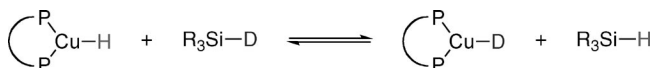
Table 2. Stoichiometric H/D labeling experiments with BINAP or DMDP as phosphane. Experimental conditions: acetophenone as substrate, toluene as solvent, reaction performed at –78 °C, *c* = 0.0125 mmol/mL.

Experiment <sup>[a]</sup>	Product H/D ratio <sup>[b]</sup>	
	BINAP	DMDP
acetophenone +  Cu–H + Ph <sub>2</sub> SiD <sub>2</sub>	64 : 36	80 : 20
acetophenone +  Cu–D + Ph <sub>2</sub> SiH <sub>2</sub>	60 : 40	24 : 76

[a] See Experimental Section for details. [b] Determined by <sup>1</sup>H NMR spectroscopy.

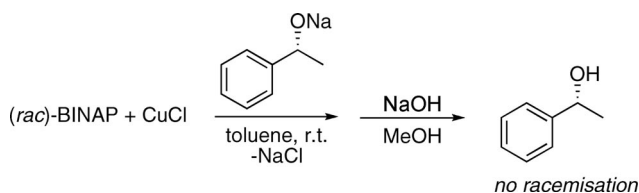






Scheme 8. H/D scrambling that may interfere with the stoichiometric labeling experiments.

**Equilibrium between Copper Alkoxide and Copper Hydride?** In the generally accepted mechanism, the copper hydride species is proposed to react with the ketone substrate by insertion of the carbonyl group into the Cu–H bond, this step determining the stereochemical outcome of the hydrosilylation reaction. The question of reversibility of this step may be of particular interest. To examine whether equilibrium exists, we reacted racemic BINAP with one equivalent of CuCl in the presence of one equivalent of sodium (*R*)-1-phenylethanol (99% *ee*) in toluene at room temperature. After stirring for three hours, diphenylsilane was added, followed by hydrolysis with a NaOH/MeOH solution (Scheme 9). The resulting solution was analyzed and no acetophenone was observed; in addition, the starting 1-phenylethanol was recovered in quantitative yield by flash chromatography. Chiral GC analysis revealed that the enantiomeric excess remained unchanged (99% *ee*), which suggests that ketone insertion into the Cu–H bond is an irreversible step.



Scheme 9. Investigation of the equilibrium between copper alkoxide and copper hydride.

## Discussion

The in situ reaction of CuCl, NaOtBu, and phosphane followed by the addition of a silane is an easy way to generate copper hydride species (Scheme 2), and this has been well documented by now.<sup>[10c]</sup> It is established that the ligand should be present prior to silane addition since nonligated Cu–H is regarded as unstable. Although there are plenty of examples of in situ generation of (phosphane)Cu–H species, only very few examples of such species have been fully characterized. We note that in the solid state only two well-defined Cu–H complexes have been characterized by X-ray crystallography (with phosphane as the supporting ligand). The (PPh<sub>3</sub>)CuH species (“Stryker reagent”)<sup>[29]</sup> was determined to be a [(PPh<sub>3</sub>)CuH]<sub>6</sub> hexamer in 1971 by Osborn.<sup>[30]</sup> Later on, Caulton found that a triphos type ligand could act as a dipode with copper to give a dimeric species.<sup>[31]</sup> We also note that, more recently, an N-heterocyclic carbene was used to stabilize Cu–H, and the resulting complex was found to be also dimeric (Figure 9).<sup>[32,33]</sup>

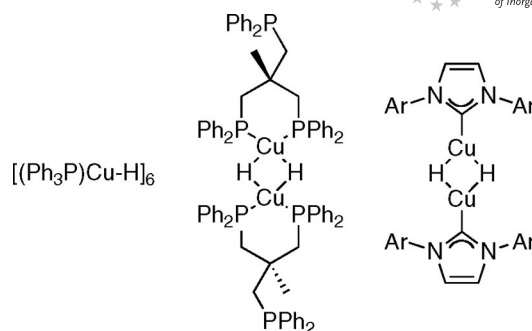


Figure 9. [LCu–H] species that have been characterized by X-ray crystallography.

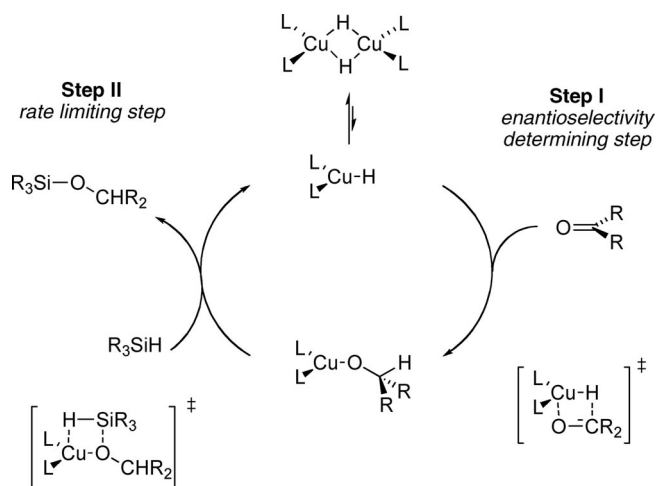
The Stryker reagent [(PPh<sub>3</sub>)CuH]<sub>6</sub> has been studied in solution, and its <sup>1</sup>H NMR spectrum displays a Cu–H hydride resonance at  $\delta = 3.52$  ppm in C<sub>6</sub>D<sub>6</sub>.<sup>[34]</sup> Lipshutz et al. highlighted the difficulty to isolate and characterize such diphosphane complexes. More recently, they studied by <sup>1</sup>H NMR spectroscopy the in situ reaction of copper acetate, PMHS, and SEGPHOS ligand and tentatively assigned a new peak at  $\delta = 2.55$  ppm as the hydride. Unlike Stryker's reagent, all attempts to locate the Cu–H with BINAP as ligand failed. Numerous attempts to crystallize such species by different techniques (layering, temperature cooling, or solvent evaporation) resulted in all cases to the formation of crystals of the free BINAP. The use of DFT calculations revealed to be much more informative.

A salient feature of these calculations is that, regardless of the modeled catalyst and the ketone, the first step of the catalytic process, that is, the insertion of the ketone into the Cu–H bond to yield an alkoxy intermediate, is rather facile, and more so than the second step involving the silane. This may appear somewhat contradictory with our experimental observations and those of Lipshutz et al., which point to the absence of reaction between a stoichiometric amount of the hydrido copper complex and the ketone.<sup>[15]</sup> We can rationalize this feature by the presence of a pre-equilibrium between the hydrido copper complex and its dimer. The calculations carried out for Cu<sub>2</sub>(μ-H)<sub>2</sub>(PH<sub>3</sub>)<sub>4</sub> and Cu<sub>2</sub>(μ-H)<sub>2</sub>–[Ph<sub>2</sub>P(C<sub>12</sub>H<sub>8</sub>)PPh<sub>2</sub>]<sub>2</sub> suggest that the dimeric form is more stable than the monomeric one by a few kcal mol<sup>–1</sup> and as stable as the alkoxy intermediate. The kinetic studies also support the formation of a dimeric [LCu–H]<sub>2</sub> species, as a half-order dependence on catalyst concentration was observed. It is noteworthy that sterically crowded diphosphane/Cu systems display higher catalytic activity, which may reflect their decreased tendency to aggregate.<sup>[10c,35]</sup>

Additional elements regarding the dimerization of the catalytically active species may be obtained from experiments in which the enantiomeric excess of the starting ligand was varied.<sup>[36]</sup> Akin to Lipshutz et al.,<sup>[15]</sup> a linear relationship between the *ee* of product and the *ee* of the ligand was observed at –78 °C and at room temperature.<sup>[37]</sup> However, the absence of a nonlinear effect may be possible if the homo- and heterochiral dimers exhibit a similar stability and if they also have an equal propensity for dissociation into catalytically active monomers.<sup>[38]</sup> According to the

DFT computations, the homochiral dimer (*R,R*) of the catalyst  $\{\text{Cu}(\text{H})[\text{Ph}_2\text{P}(\text{C}_{12}\text{H}_8)\text{PPh}_2]\}_2$  (**1d**) is more stable than the heterochiral dimer (*R,S*) (Figure 7) by only 4.5 kcal mol<sup>-1</sup>. This confirms the assumption that the homo- and heterochiral dimers exhibit a similar stability, as observed in dialkylzinc addition to benzaldehyde<sup>[39]</sup> and accounts for the absence of nonlinear effects.

Scheme 10 displays the overall catalytic cycle as deduced from our theoretical studies. These results suggest that ketone insertion is the enantioselectivity determining step (Step I). Further calculations with acetophenone as the ketone substrate showed that the (*R*) configuration of BINAP would favor the diastereomeric form that give rise to the (*R*)-1-phenylethanol, which is consistent with the experimental results (see Figure 4).<sup>[40]</sup> However, this step would be the enantioselectivity determining step only if the reaction is irreversible, which appears to be the case on the basis of the in situ reaction of racemic BINAP, CuCl, and enantiopure sodium (*R*)-1-phenylethanol. An equilibrium between the copper alkoxide and the copper hydride would lead to a racemization of the alkoxide, which is not observed in the present case.<sup>[41]</sup>



Scheme 10. Catalytic cycle displaying the two steps in the copper-catalyzed hydrosilylation process.

Step II, which corresponds to the reaction of the copper alkoxide with the silane to form the silyl product and regenerate copper hydride, is found to be the rate determining step. Investigation of the kinetic isotope effect in the hydrosilylation of acetophenone also supports this step as the rate limiting one. Thus, the  $k_{\text{H}}/k_{\text{D}}$  value of 2 is consistent with the interaction of Cu alkoxide with the Si–H bond to yield the product and regenerate the Cu–H species via transition state **TS2**.<sup>[42]</sup> The free energy barriers computed for the model systems may be considered somewhat too high if one takes into account the fact that, experimentally, the overall reaction seems to occur rather easily. We have already mentioned that the inclusion of the entropic effects with the underlying assumption that all molecules are in the gas phase leads to an entropy decrease that is too large for associative processes and therefore to free energy differences that are too positive. Another factor might be the use of

$\text{SiMe}_2\text{H}_2$  to model the silane. The silanes that are used experimentally all bear at least one aryl group, which might give rise to some additional stabilizing interactions.

We finally conducted an isotope labeling experiment that allowed us to follow the hydride pathway in the Cu–H species. Stoichiometric reaction of in situ generated LCu–H with acetophenone, followed by addition of one equivalent of hydrogenated silane, leads to incorporation of deuterium in the product, whereas reaction of LCu–D with acetophenone, followed by addition of one equivalent of deuteriated silane, leads to incorporation of hydrogen in the product (Scheme 7). In addition, the latter experiment also ruled out our originally postulated intermediates displayed in Scheme 4.

## Conclusions

The combination of theoretical and experimental studies provides a insightful mechanistic proposal for the enantioselective hydrosilylation of ketones catalyzed by copper diphosphane complexes. The data presented here support a mechanism in which the rate limiting step is the formation of the silyl ether product and concomitant regeneration of copper hydride species. On the other hand, the enantioselectivity determining step is the reaction of the prochiral ketone with the copper hydride species. The fact that the copper hydride species does not react with a stoichiometric amount of ketone may be due to aggregation of the Cu–H species. Thus, the reaction occurs only in the presence of a silane, which is the driving force of the reaction leading to the formation of a stable silyl ether product.

## Experimental Section

### Computational Details

The calculations were carried out at the DFT-B3LYP level<sup>[43]</sup> with the Gaussian 03 program.<sup>[44]</sup> The geometries of the reactants, products, intermediates, and transition states were optimized by the gradient technique, using first the 6-31G\*\* basis set<sup>[45]</sup> for the nonmetallic atoms and for Cu, the Karlsruhe def2-SVP basis set,<sup>[46]</sup> which we modified slightly by contraction of the 5d GTO set [3,1,1] in a TZ type fashion, following an earlier recommendation of Ahlrichs et al.<sup>[47]</sup> This basis set will be referred to as BS-I. The nature of the optimized structures, either transition states or intermediates, was assessed through a frequency calculation. The changes of Gibbs free reaction energies were obtained by taking into account zero-point energies, thermal motion, and the entropy contribution at standard conditions (temperature 298.15 K, pressure 1 atm) from the B3LYP/BSI//B3LYP/BSI calculations.

We tested the effects of larger basis sets in pilot calculations and for some selected intermediates and transition states of the catalytic cycle (vide supra). We first combined the 6-311++G\*\* for the nonmetallic atoms<sup>[48]</sup> with either the Karlsruhe def2-TZVP basis set (BS-II) or the Stuttgart quasi-relativistic pseudopotential and SDD basis set of Dolg et al. for Cu (BS-III).<sup>[49]</sup> We also checked the TZVP basis set<sup>[50]</sup> for all atoms (BSIV), which was used by Oestreich et al. in their recent theoretical study of the copper-catalyzed alcohol silylation.<sup>[51]</sup> Either the optimized geometries or the ener-

getic results turned out to be quite similar. Finally, single-point CCSD(T) calculations (which can be considered as state of the art calculations) were carried out for a few intermediates and transition states involving the smallest catalyst **1a**. Here too, the energy differences were not severely affected. We will therefore concentrate our discussion on the B3LYP/BS-I results.

**General Procedures:** All experiments were carried out under N<sub>2</sub> by using standard Schlenk techniques or in a MBraun Unilab glovebox. THF, dichloromethane, and toluene were first dried through a solvent purification system (MBraun SPS) and stored for at least a couple of days over activated molecular sieves (4 Å) in a glovebox prior to use. CD<sub>2</sub>Cl<sub>2</sub> and C<sub>6</sub>D<sub>6</sub> were purchased from Eurisotope (CEA, Saclay, France), degassed under a N<sub>2</sub> flow, and stored over activated molecular sieves (4 Å) in a glovebox prior to use. (*R*)-1-phenylethanol was purchased from Fluka. DMDP phosphane was provided by Clariant (Huningue). NMR spectra were recorded with Bruker AC 300 or 400 MHz NMR spectrometers. <sup>1</sup>H and <sup>13</sup>C NMR chemical shifts are reported vs. SiMe<sub>4</sub> and were determined by reference to the residual <sup>1</sup>H and <sup>13</sup>C solvent peaks. Gas chromatography analysis was performed with a chiral capillary column Chiraldex B-PM, 50 m × 0.25 mm.

**Representative Procedure for the Hydrosilylation of Acetophenone:** (Example from Figure 1) A Schlenk tube was charged with CuCl (0.025 mmol), NaO-*t*Bu (0.025 mmol), and (*R*)-BINAP (0.025 mmol). Dry toluene (5.0 mL) was added under argon, and the solution was stirred for 20 min at room temperature. After cooling to –78 °C, the silane (PhMeSiH<sub>2</sub>, 1.0 mmol) was added dropwise, followed by the acetophenone (0.5 mmol). The yellow solution was stirred at –78 °C for 16 h. Upon completion of the reaction, a solution of NaOH in methanol was added (2 mL, 1.0 M), and the resulting mixture was stirred for 1 h at room temperature. Column chromatography provided the desired alcohol (60.4 mg, 99% yield). GC analysis on a chiral column gave a 93% *ee* (*R*). The absolute configuration was determined by comparison of the optical rotation with literature values.

**Kinetic Studies:** Hydrosilylation studies were carried out at 298 K with [D<sub>6</sub>]benzene as solvent. The general procedure was followed, and the solution was transferred into an NMR tube with a Teflon valve. The sample was allowed to stand at 298 K before the desired silane was added at *t*<sub>0</sub>. The progress of the reaction was monitored by measuring the disappearance of the ketone and the appearance of the product by <sup>1</sup>H NMR spectroscopy. The initial rates of the various reactions were determined from an exponential fitting analysis of the conversion curves.

**Kinetic Isotope Effect:** The general procedure for the hydrosilylation of acetophenone was followed, and a 1:1 ratio stock solution of the silane (Ph<sub>2</sub>SiH<sub>2</sub>) and the deuteriosilane (Ph<sub>2</sub>SiD<sub>2</sub>) was used. The crude mixture and the purified product were used to measure the ratio of nondeuteriated and deuteriated products by comparing the integrations in the <sup>1</sup>H NMR spectrum of PhCH(OZ)CH<sub>3</sub> (q at δ = 4.78 ppm) and PhCH(OZ)CH<sub>3</sub> + PhCD(OZ)CH<sub>3</sub> (*pseudo-s+d* at δ = 1.38 ppm). Independently, the initial rates of hydrosilylation of acetophenone were determined with Ph<sub>2</sub>SiH<sub>2</sub> or Ph<sub>2</sub>SiD<sub>2</sub> as silane and by using the representative procedure.

**Isotope Labeling (Representative Procedure):** In the glove box, a Schlenk tube was charged with CuCl (0.25 mmol), NaO*t*Bu (0.25 mmol), DMDP (0.25 mmol), and dry toluene (20 mL). The Schlenk tube, equipped with a stirring bar and a septum cap, was then taken out of the glove box, and the solution was stirred for 30 min at room temperature. The desired silane (Ph<sub>2</sub>SiD<sub>2</sub>, 0.25 mmol) was added dropwise, and the resulting solution was

stirred for 2 h at room temperature (the color changed to yellow). The Schlenk tube was then cooled to –78 °C, and acetophenone followed by Ph<sub>2</sub>SiH<sub>2</sub> (0.25 mmol each) were added. The resulting solution was allowed to react at this temperature for 1 h. A solution of NaOH in methanol was added, and the resulting mixture was stirred for 1 h at room temperature. After evaporation of the solvents, the product was purified by flash column chromatography, which afforded 1-phenylethanol in 98% yield. The H/D ratio was determined by <sup>1</sup>H NMR spectroscopy, which revealed 76% of deuterium incorporation.

**Racemization Experiment with Enantioenriched 1-Phenylethanol:** In a glove box, a Schlenk tube was charged with CuCl (0.25 mmol), racemic-BINAP (0.25 mmol), and sodium (*R*)-1-phenylethanol (99% *ee*). Dry toluene (20 mL) was added, and the resulting solution was stirred for 3 h (the color changed to yellow, and a white precipitate appeared). Diphenylsilane (0.3 mmol) was added followed, after 30 min, by a solution of NaOH in MeOH. After evaporation of the solvents, the crude product was purified by flash column chromatography to give the 1-phenylethanol in 94% yield. Chiral GC analysis revealed an >99% *ee*.

**Supporting Information** (see footnote on the first page of this article): Experimental details for the kinetic studies, plot of observed *ee* of product as a function of *ee* of the ligand, influence of the temperature on the selectivity. Tables of energies and Cartesian coordinates for all structures (XYZ).

## Acknowledgments

We thank the Centre National de la Recherche Scientifique (CNRS) and the Ministère de l'Éducation Nationale, de la Recherche et de la Technologie for a Ph.D. grant (to J. T. I. and F.-P. N.) and an Action Concertée Incitative (ACI) Jeunes chercheuses et jeunes chercheurs grant. The calculations have been carried out on the workstation of the Laboratoire de Chimie Quantique and the IDRIS Orsay. We thank S. Fersing for her technical assistance.

- [1] E. N. Jacobsen, A. Pfaltz, H. Yamamoto (Eds.), *Comprehensive Asymmetric Catalysis*, Springer-Verlag, New York, 1999.
- [2] H. Nishiyama, K. Itoh, *Catalytic Asymmetric Synthesis* (Ed.: I. Ojima), Wiley-VCH, New York, 2000, ch. 2.
- [3] a) I. Ojima, M. Nihonyanagi, Y. Nagai, *J. Chem. Soc., Chem. Commun.* 1972, 938; b) R. J. P. Corriu, J. J. E. Moreau, *J. Chem. Soc., Chem. Commun.* 1973, 38; c) W. Dumont, J. C. Poulin, T.-P. Dang, H. B. Kagan, *J. Am. Chem. Soc.* 1973, 95, 8295.
- [4] Selected examples: a) H. Nishiyama, H. Sakaguchi, T. Nakamura, M. Horiata, M. Kondo, K. Itoh, *Organometallics* 1989, 8, 846; b) M. Sawamura, R. Kuwano, Y. Ito, *Angew. Chem. Int. Ed. Engl.* 1994, 33, 111; c) A. Sudo, H. Yoshida, K. Saigo, *Tetrahedron: Asymmetry* 1997, 8, 3205; d) B. Tao, G. C. Fu, *Angew. Chem. Int. Ed.* 2002, 41, 3892; e) D. A. Evans, F. E. Michael, J. S. Tedrow, K. R. Campos, *J. Am. Chem. Soc.* 2003, 125, 3534; f) V. César, S. Bellemin-Laponnaz, H. Wade, L. H. Gade, *Chem. Eur. J.* 2005, 11, 2862.
- [5] For mechanistic investigations of rhodium-catalyzed hydrosilylation of ketones, see: a) I. Ojima, T. Kogure, M. Kumagai, S. Horiuchi, Y. Sato, *J. Organomet. Chem.* 1976, 122, 83; b) G. Z. Zheng, T. H. Chan, *Organometallics* 1995, 14, 70; c) C. Reyes, A. Prock, W. P. Giering, *Organometallics* 2002, 21, 546; d) N. Schneider, M. Finger, C. Haferkemper, S. Bellemin-Laponnaz, P. Hofmann, L. H. Gade, *Angew. Chem. Int. Ed.* 2009, 48, 1609; e) N. Schneider, M. Finger, C. Haferkemper, S. Bellemin-Laponnaz, P. Hofmann, L. H. Gade, *Chem. Eur. J.* 2009, 15, 11515.



- [6] a) G. Zhu, M. Terry, X. Zhang, *J. Organomet. Chem.* **1997**, 547, 97; b) Y. Nishibayashi, I. Takei, S. Uemura, M. Hidai, *Organometallics* **1998**, 17, 3420; c) C. Moreau, C. G. Frost, B. Murrer, *Tetrahedron Lett.* **1999**, 40, 5617.
- [7] a) H. Mimoun, J. Y. de Saint Laumer, L. Giannini, R. Scopelitti, C. Floriani, *J. Am. Chem. Soc.* **1999**, 121, 6158; b) V. Bette, A. Mortreux, D. Savoia, J.-F. Carpentier, *Tetrahedron* **2004**, 60, 2837; c) V. Bette, A. Mortreux, D. Savoia, J.-F. Carpentier, *Adv. Synth. Catal.* **2005**, 347, 289.
- [8] J. Yun, S. L. Buchwald, *J. Am. Chem. Soc.* **1999**, 121, 5640.
- [9] a) B. K. Langlotz, H. Wadepohl, L. H. Gade, *Angew. Chem. Int. Ed.* **2008**, 47, 4670; b) N. S. Shaikh, S. Enthaler, K. Junge, M. Beller, *Angew. Chem. Int. Ed.* **2008**, 47, 2497.
- [10] For reviews on hydrosilylation of ketones, see: a) J.-F. Carpentier, V. Bette, *Curr. Org. Chem.* **2002**, 6, 913; b) O. Riant, N. Mostefaï, J. Courmacel, *Synthesis* **2004**, 2943; c) C. Deutsch, N. Krause, B. H. Lipshutz, *Chem. Rev.* **2008**, 108, 2916; d) S. Díez-González, S. P. Nolan, *Acc. Chem. Res.* **2008**, 41, 349.
- [11] H. Brunner, W. Miehling, *J. Organomet. Chem.* **1984**, 275, C17.1.
- [12] B. H. Lipshutz, K. Noson, W. Chrisman, *J. Am. Chem. Soc.* **2001**, 123, 12917.
- [13] For other examples of copper-based systems for asymmetric hydrosilylation of ketones, see: a) S. Sirol, J. Courmacel, N. Mostefaï, O. Riant, *Org. Lett.* **2001**, 3, 4111; b) J. Courmacel, N. Mostefaï, S. Sirol, S. Chopin, O. Riant, *Isr. J. Chem.* **2002**, 41, 231; c) D.-w. Lee, J. Yun, *Tetrahedron Lett.* **2004**, 45, 5415; d) J. Wu, J.-X. Ji, A. S. C. Chan, *Proc. Natl. Acad. Sci. USA* **2005**, 102, 3570; e) M. L. Kantam, S. Laha, J. Yadav, P. R. Likhar, B. Sreedhar, B. M. Choudary, *Adv. Synth. Catal.* **2007**, 349, 1797; f) N. Mostefaï, S. Sirol, J. Courmacel, O. Riant, *Synthesis* **2007**, 8, 1265; g) M. L. Kantam, S. Laha, J. Yadav, P. R. Likhar, B. Sreedhar, S. Jha, S. Bhargava, M. Udayakiran, B. Jagadeesh, *Org. Lett.* **2008**, 10, 2979.
- [14] a) D. H. Appella, Y. Moritani, R. Shintani, E. M. Ferreira, S. L. Buchwald, *J. Am. Chem. Soc.* **1999**, 121, 9473; b) Y. Moritani, D. H. Appella, V. Jurkauskas, S. L. Buchwald, *J. Am. Chem. Soc.* **2000**, 122, 6797.
- [15] B. H. Lipshutz, K. Noson, W. Chrisman, A. Lower, *J. Am. Chem. Soc.* **2003**, 125, 8779.
- [16] J. T. Issenhardt, S. Dagorne, S. Bellemin-Laponnaz, *Adv. Synth. Catal.* **2006**, 348, 1991.
- [17] H. Ito, T. Ishizuka, T. Okumura, H. Yamanaka, J. Tateiwa, M. Sonoda, A. Hosomi, *J. Organomet. Chem.* **1999**, 574, 102.
- [18] Two different diphosphate ligands were used in this study: 2,2'-bis(diphenylphosphanyl)-1,1'-binaphthyl (BINAP) and 2,2-dimethyl-1,3-bis(diphenylphosphanyl)propane (DMDP).
- [19] F. P. Notter, Ph. D. Thesis, Université de Strasbourg, **2008**.
- [20] a) H. Tamura, H. Yamasaki, H. Sato, S. Sakaki, *J. Am. Chem. Soc.* **2003**, 125, 16114; b) S. Sakaki, T. Takayama, M. Sumimoto, M. Sugimoto, *J. Am. Chem. Soc.* **2004**, 126, 3332; c) M. Sumimoto, N. Iwane, T. Takahama, S. Sakaki, *J. Am. Chem. Soc.* **2004**, 126, 10457; d) B. O. Leung, D. L. Reid, D. A. Armstrong, A. Rauk, *J. Phys. Chem. A* **2004**, 108, 2720; e) A. A. C. Braga, G. Ujaque, F. Maseras, *Organometallics* **2006**, 25, 3647; f) P. Deglmann, E. Ember, P. Hofmann, S. Pitter, O. Walter, *Chem. Eur. J.* **2007**, 13, 2864.
- [21] S. C. A. H. Pierrefixe, F. M. Bickelhaupt, *Struct. Chem.* **2007**, 18, 813.
- [22] R. Hoffmann, J. M. Howell, E. L. Muetterties, *J. Am. Chem. Soc.* **1972**, 94, 3047.
- [23] S. C. A. Y. Pierrefixe, C. F. Guerra, F. M. Bickelhaupt, *Chem. Eur. J.* **2008**, 14, 819.
- [24] M. Onda, Y. Kohama, K. Suga, I. Yamaguchi, *J. Mol. Struct.* **1998**, 442, 19.
- [25] G. De Luca, M. Longeri, G. Pileio, P. Lantto, *ChemPhysChem* **2005**, 6, 2086.
- [26] a) T. Miyahara, T. Inazu, *THEOCHEM* **1996**, 364, 131; b) A. N. Rodriguez, F. A. Giannini, H. A. Baldoni, L. N. Santa-gata, M. A. Zamora, S. Zacchino, C. P. Sosa, R. D. Enriz, I. G. Csizmadia, *THEOCHEM* **1999**, 463, 271.
- [27] P. Milko, J. Roithova, D. Schröder, J. Lemaire, H. Schwarz, M. C. Holthausen, *Chem. Eur. J.* **2008**, 14, 4318.
- [28] T.-H. Chan, A. Melnyk, *J. Am. Chem. Soc.* **1970**, 92, 3718.
- [29] J.-X. Chen, J. F. Daeuble, D. M. Brestensky, J. M. Stryker, *Tetrahedron* **2000**, 56, 2153.
- [30] a) M. R. Churchill, S. A. Bezman, J. A. Osborn, J. Wormald, *Inorg. Chem.* **1972**, 11, 1818; b) T. H. Lemmen, K. Foltz, J. C. Huffman, K. G. Caulton, *J. Am. Chem. Soc.* **1985**, 107, 7774.
- [31] G. V. Goeden, J. C. Huffman, K. G. Caulton, *Inorg. Chem.* **1986**, 25, 2484.
- [32] N. P. Mankad, D. S. Laitar, J. P. Sadighi, *Organometallics* **2004**, 23, 3369–3371.
- [33] NHC ligands offer low kinetic lability with transition metals. Thus, several copper(I) species have been fully characterized by coordination of NHC ligands to the metal center. See ref.<sup>[32]</sup> and for example: a) L. A. Goj, E. D. Blue, C. Munro-Leighton, T. B. Gunnoe, J. L. Petersen, *Inorg. Chem.* **2005**, 44, 8647–8649; b) L. A. Goj, E. D. Blue, S. A. Delp, T. B. Gunnoe, T. R. Cundari, A. W. Pierpont, J. L. Petersen, P. D. Boyle, *Inorg. Chem.* **2006**, 45, 9032–9045; c) K. X. Bhattacharyya, J. A. Akana, D. S. Laitar, J. M. Berlin, J. P. Sadighi, *Organometallics* **2008**, 27, 2682–2684; NHC ligands have allowed complete characterization of monomeric gold(I) hydride complexes, see: d) E. Y. Tsui, P. Müller, J. P. Sadighi, *Angew. Chem. Int. Ed.* **2008**, 47, 8937–8940.
- [34] G. V. Goeden, K. G. Caulton, *J. Am. Chem. Soc.* **1981**, 103, 7354.
- [35] Stryker and collaborators also suggested that the active species in the ketone reduction with  $[(\text{Ph}_3\text{P})\text{CuH}]_6$  is probably at a lower aggregate (possibly monomeric), see: a) W. S. Mahoney, J. M. Stryker, *J. Am. Chem. Soc.* **1989**, 111, 8818; b) J.-X. Chen, J. F. Daeuble, D. M. Brestensky, J. M. Stryker, *Tetrahedron* **2000**, 56, 2153.
- [36] T. Satyanarayana, S. Abraham, H. B. Kagan, *Angew. Chem. Int. Ed.* **2009**, 48, 456.
- [37]  $\text{CuCl}/\text{NaOt-Bu}/\text{BINAP}$  as catalytic system (5 mol-%), acetophenone as substrate,  $\text{PhMeSiH}_2$  as silane: see data in Supporting Information
- [38] M. Kitamura, S. Suga, H. Oka, R. Noyori, *J. Am. Chem. Soc.* **1998**, 120, 9800.
- [39] Goldfuss and collaborators observed a linear relationship between the *ee* of product and that of ligand in the case of dialkylzinc additions to benzaldehyde using chiral anisyl fenchols. Ab initio calculations of homo- and heterochiral dimers revealed energy differences up to 3.0 kcal mol<sup>-1</sup>, see: M. Steigelmann, Y. Nisar, F. Rominger, B. Goldfuss, *Chem. Eur. J.* **2002**, 8, 5211.
- [40] We are well aware however that the DFT calculations may not take properly into account weak interactions such as  $\pi$ - $\pi$  interactions or  $\text{CH}/\pi$  interactions. Thus the agreement between theory and experiment may be regarded as fortuitous. Yet the overall consistency of the experimental and theoretical results adds credence to our final conclusions.
- [41] Note that Osakada et al. studied the stability of copper alkoxide  $(\text{Ph}_3\text{P})_3\text{Cu-OCHPh}_2$  and found that decomposition by thermolysis (at 200 °C for 20 min) of the complex could lead to a mixture of benzophenone and diphenylmethanol, see: K. Osakada, T. Takizawa, M. Tanaka, T. Yamamoto, *J. Organomet. Chem.* **1994**, 473, 359.
- [42] A catalytic cycle that contains an enantioselectivity determining step different from the rate limiting step was also postulated for the titanium-catalyzed hydrosilylation of ketones. The hypothesis was proposed based on the rate enhancement when alcohol was added to the reaction mixture. Such a positive alcohol effect was also observed in some cases with copper hydride-catalyzed reactions, see references 8 and 10c.

- [43] a) A. D. Becke, *Phys. Rev. A* **1988**, 38, 3098; b) C. Lee, W. Yang, R. G. Parr, *Phys. Rev. B* **1988**, 37, 785; c) A. D. Becke, *J. Chem. Phys.* **1993**, 98, 5648.
- [44] M. J. Frisch, G. W. Trucks, H. B. Schlegel, G. E. Scuseria, M. A. Robb, J. R. Cheeseman, J. A. Montgomery Jr., T. Vreven, K. N. Kudin, J. C. Burant, J. M. Millam, S. S. Iyengar, J. Tomasi, V. Barone, B. Mennucci, M. Cossi, G. Scalmani, N. Rega, G. A. Petersson, H. Nakatsuji, M. Hada, M. Ehara, K. Toyota, R. Fukuda, J. Hasegawa, M. Ishida, T. Nakajima, Y. Honda, O. Kitao, H. Nakai, M. Klene, X. Li, J. E. Knox, H. P. Hratchian, J. B. Cross, V. Bakken, C. Adamo, J. Jaramillo, R. Gomperts, R. E. Stratmann, O. Yazyev, A. J. Austin, R. Cammi, C. Pomelli, J. W. Ochterski, P. Y. Ayala, K. Morokuma, G. A. Voth, P. Salvador, J. J. Dannenberg, V. G. Zakrzewski, S. Dapprich, A. D. Daniels, M. C. Strain, O. Farkas, D. K. Malick, A. D. Rabuck, K. Raghavachari, J. B. Foresman, J. V. Ortiz, Q. Cui, A. G. Baboul, S. Clifford, J. Cioslowski, B. B. Stefanov, G. Liu, A. Liashenko, P. Piskorz, I. Komaromi, R. L. Martin, D. J. Fox, T. Keith, M. A. Al-Laham, C. Y. Peng, A. Nanayakkara, M. Challacombe, P. M. W. Gill, B. Johnson, W. Chen, M. W. Wong, C. Gonzalez, J. A. Pople, *Gaussian 03*, Revision B.04 ed., Gaussian, Inc., Pittsburgh, PA, **2003**.
- [45] a) P. C. Hariharan, J. A. Pople, *Mol. Phys.* **1974**, 27, 209; b) P. C. Hariharan, J. A. Pople, *Chem. Phys. Lett.* **1972**, 16, 217.
- [46] F. Weigend, R. Ahlrichs, *Phys. Chem. Chem. Phys.* **2005**, 7, 3297.
- [47] A. Schäfer, H. Horn, R. Ahlrichs, *J. Chem. Phys.* **1992**, 97, 2571.
- [48] R. Krishnan, J. S. Binkley, R. Seeger, J. A. Pople, *J. Chem. Phys.* **1980**, 72, 650.
- [49] D. Andrae, U. Häussermann, M. Dolg, H. Stoll, H. Preuss, *Theor. Chim. Acta* **1990**, 77, 123.
- [50] A. Schäfer, R. Huber, R. Ahlrichs, *J. Chem. Phys.* **1994**, 100, 5829.
- [51] S. Rendler, O. Plefka, B. Karatas, G. Auer, R. Fröhlich, C. Mück-Lichtenfeld, S. Grimme, M. Oestreich, *Chem. Eur. J.* **2008**, 14, 11512–11528.

Received: September 28, 2009

Published Online: November 30, 2009